5. MOST Project - 2

(9) INFORMAL MANUSCRIPT REPORT

NO. [redacted]

(14) N00-IM-0-33-

(6) TITLE

THEORETICAL COMPUTATIONS OF SOUND REFLECTION FROM A LAYERED OCEAN BOTTOM.

(12) 24p.

AUTHOR

(10) ROBERT S. WINOKUR

DATE

(11) OCT [redacted]65

This manuscript has a limited distribution, therefore in citing it in a bibliography, the reference should be followed by the phrase UNPUBLISHED MANUSCRIPT.

MARINE SCIENCES DEPARTMENT
U. S. NAVAL OCEANOGRAPHIC OFFICE
WASHINGTON, D. C. 20390

PREFACE

This paper was prepared for presentation at the seminar on Sound Ray Tracing and Isointensity Contours in the Ocean at Pennsylvania State University and delivered by the author the week of July 12, 1965.

Letter on file

TABLE OF CONTENTS

FIGURES

THEORETICAL COMPUTATIONS OF SOUND REFLECTION FROM A LAYERED OCEAN BOTTOM

INTRODUCTION

The U. S. Naval Oceanographic Office is engaged in a program to determine the influence of bottom composition, structure, and topography on sound reflection from the ocean bottom. As one step towards accomplishing this objective, a computer program was prepared to enable theoretical investigations of the effect of layered sediments on sound reflection. The computer mathematical model permits detailed and systematic calculations of bottom reflection coefficients and bottom reflection loss as the following factors are varied parametrically: number of reflecting layers, layer thickness, sediment sound velocity, density, sediment absorption, and frequency. This paper will illustrate how a layered ocean bottom model can be used to develop an understanding of ocean bottom reflectivity.

DESCRIPTION OF COMPUTER PROGRAM

The computer program computes the complex reflection coefficient, phase shift, and reflection loss for a plane wave obliquely incident on a layered absorbing bottom. Expressions for the reflection coefficient are derived from the wave equation by utilizing steady state solutions to the differential equation for a "Voigt Liquid." Matrix algebraic operations after the method of Haskell (1) are employed.

The mathematical derivation assumes a multilayered ocean bottom in which the sediment layer thickness (D), sound velocity (C), density (ρ), and absorption (a) are assigned arbitrary values. The number of layers considered is not limited and the lowermost layer in the sedimentary sequence is considered to be semi-infinite. The sedimentary layers are assumed to be fluid; that is, the shear modulus $\mu = 0$. The layers are further assumed to be absorbing and to have plane parallel interfaces. The pressure and particle velocity are continuous across the interfaces between the layers.

The computer program was developed and written by Dr. James Dorman, as a consultant to Alpine Geophysical Associates (2), under contract to the U. S. Naval Oceanographic Office. A detailed discussion of the theory involved in the development of the program can be found in reference (2). The following equations are presented as background information as the fundamental relationships utilized in developing the layered model.

The velocity potential of compressional waves that travel in the fluid must satisfy the differential equation for a "Voigt Liquid,"

$$\rho \frac{\partial^2 \phi}{\partial t^2} = \lambda \nabla^2 \phi + \lambda' \frac{\partial}{\partial t} \nabla^2 \phi, \tag{1a}$$

or

$$\frac{\partial^2 \phi}{\partial t^2} = a^2 \nabla^2 \phi + a'^2 \frac{\partial}{\partial t} \nabla^2 \phi, \quad a^2 = \frac{\lambda}{\rho}, \; a'^2 = \frac{\lambda'}{\rho} \tag{1b}$$

A solution of the differential equation is

$$\phi = (A, A') \exp(i\omega t) \begin{bmatrix} \exp\left[-i\zeta (x + z \tan\theta)\right] \\ \exp\left[-i\zeta (x - z \tan\theta)\right] \end{bmatrix} \tag{2}$$

where the terms of ϕ containing A and A' represent oblique downgoing and upgoing waves, respectively, and $x \pm z \tan\theta$ represents the horizontal distance the wave front travels in time t.

Substituting equation 2 in equation 1b leads to

$$\omega^2 = \zeta^2 (a^2 + i\omega a'^2)(1 + \tan^2\theta). \tag{3}$$

This equation is satisfied by complex ζ. Substituting $\zeta = k + i\tau$ in equation 3 yields

$$k^2 = \frac{\omega^2}{a^2} \cos^2\theta \, \frac{\left[1 + \left(\frac{\omega a'^2}{a^2}\right)^2\right]^{1/2} + 1}{2\left[1 + \left(\frac{\omega a'^2}{a^2}\right)^2\right]}$$

and (4)

$$\tau^2 = \frac{\omega^2}{a^2} \cos^2\theta \, \frac{\left[1 + \left(\frac{\omega a'^2}{a^2}\right)^2\right]^{1/2} - 1}{2\left[1 + \left(\frac{\omega a'^2}{a^2}\right)^2\right]}$$

where the negative root of τ is taken to represent attenuation in the direction of propagation and the positive root of k represents the horizontal wave number.

The expression for the velocity potential is used to write a matrix to solve for the downward particle velocity and fluid pressure. By matrix inversion an expression for a fluid layer with Voigt-type attenuation is arrived at, and by means of recurrent matrices the reflection coefficient for an acoustic wave reflected from n layers is determined.

The computer program was written in Fortran II for an IBM 7074 computer. There are two types of input cards for the program. The first type specifies the four parameters of each layer and one card per layer is used. The parameters specified are layer thickness, layer sound velocity, density, and absorption. The absorption constant is specified as an amplitude per unit length, such as decibels per meter.

The second type of card is a frequency card which specifies the frequency in cycles per second.

All layer cards occurring in a continuous sequence are considered to be layers of a single model. The first card is treated as the first layer below the ocean bottom and the last card is treated as a semi-infinite half space. The sound velocity and density of the water layer are fixed in the program but may be readily changed to any values.

The output consists of completely annotated tables of reflection coefficients, phase shifts, and reflection loss at grazing angle intervals of 1 degree. This interval may be easily changed as desired.

TYPICAL COMPUTED CURVES

All of the computed curves illustrated in Figures 1 to 11 were arrived at by assuming or inventing typical ocean bottom conditions. The values used for sediment sound velocity are consistent with the data of Hamilton et al. (3), Shumway (4), and Sutton et al. (5). This was done to facilitate the computations and to permit each of the specified variables to be varied parametrically. By so doing a systematic investigation of the effect of frequency, sediment sound velocity, layer thickness, absorption, and the number of reflecting layers on sound reflection from the ocean bottom can be performed. While it is apparent that many combinations of these variables may exist it is possible, at this time, to present only a limited number. Each of the figures presents curves of bottom reflection loss as a function of grazing angle for a given set of conditions. The following units should be used when referring to the illustrations: sound velocity (C) in feet per second, density (ρ) in grams per cubic centimeter, layer thickness (D) in feet, and absorption (a) in decibels per foot.

Figures 1 to 6 represent computed loss values for a three layer model in which the thickness of the second layer was arbitrarily specified as 5 feet. In addition, for this model the bottom was assumed to be nonabsorbing ($a = 0$). In all cases the first layer specified (layer 1) represents the semi-infinite water layer overlying the first sediment layer (layer 2).

The dependence of bottom reflection loss on frequency for a layered ocean bottom can be seen in Figures 1 and 2. A comparison of the 1, 4, and 12 kc traces in these figures shows that as frequency increases reflection loss becomes more dependent on grazing angle. The observed dependence results from interference effects produced by reflections from the water-sediment interface and from the subbottom layer, and is seen to occur as fluctuations in the reflection loss curve as a function of grazing angle. In Figure 1 the 1 kc curve appears as a smoothly oscillating curve with 2 peaks; the 4 kc curve has 6 peaks; and the 12 kc curve is rapidly oscillating with 18 peaks. The variations in reflection loss with grazing angle range from a low of 5 decibels at 1 kc to a high of about 18 decibels at 12 kc. Since the bottom was specified to be nonabsorbing, total reflection occurs at the critical angle. Figure 1 represents a model where C_3 is the maximum velocity and C_2 the minimum velocity ($C_3 > C_1 > C_2$), while in Figure 2 C_2 is the maximum velocity and C_3 the minimum ($C_2 > C_1 > C_3$). The same frequency dependence illustrated in Figure 1 is seen in Figure 2, but the amplitude of the fluctuations is not as large. The maximum variation is about 8 decibels and at a grazing angle of about 35 degrees the oscillations are almost completely dampened. These figures indicate that a layered ocean bottom can explain fluctuations in bottom reflection loss as a function of grazing angle and that, for a nonabsorbing bottom, reflection loss data need not exhibit a uniform dependence on frequency.

The effect of sound velocity variations in layer 3 (C_3) can be estimated from an examination of Figures 3 and 4. Except for shifts in the critical angle the shape of the curves remains relatively the same as C_3 increases; however, there are noticeable differences in the amplitude of the fluctuations that appear to be controlled by C_3. It can be seen in Figure 3 that for angles less than 30 degrees the reflection loss increases for decreasing values of C_3. A transition zone is observed at 30 degrees. For angles greater than this the amplitude of the oscillations increase as C_3 increases and the maximum and minimum loss values, in this region, are associated with increasing C_3. The smooth curve in this figure represents a two layer model formed by layers 1 and 3 for $C_3 = 5200$ feet/second. It is apparent that the two layer model determines the minimum loss or lower limit of the three layer case. It should be noted that C_2 is the minimum velocity in Figure 3, whereas C_1 is the minimum in Figure 4. Figure 4 more dramatically illustrates the increase in the amplitude of the fluctuations as C_3 increases.

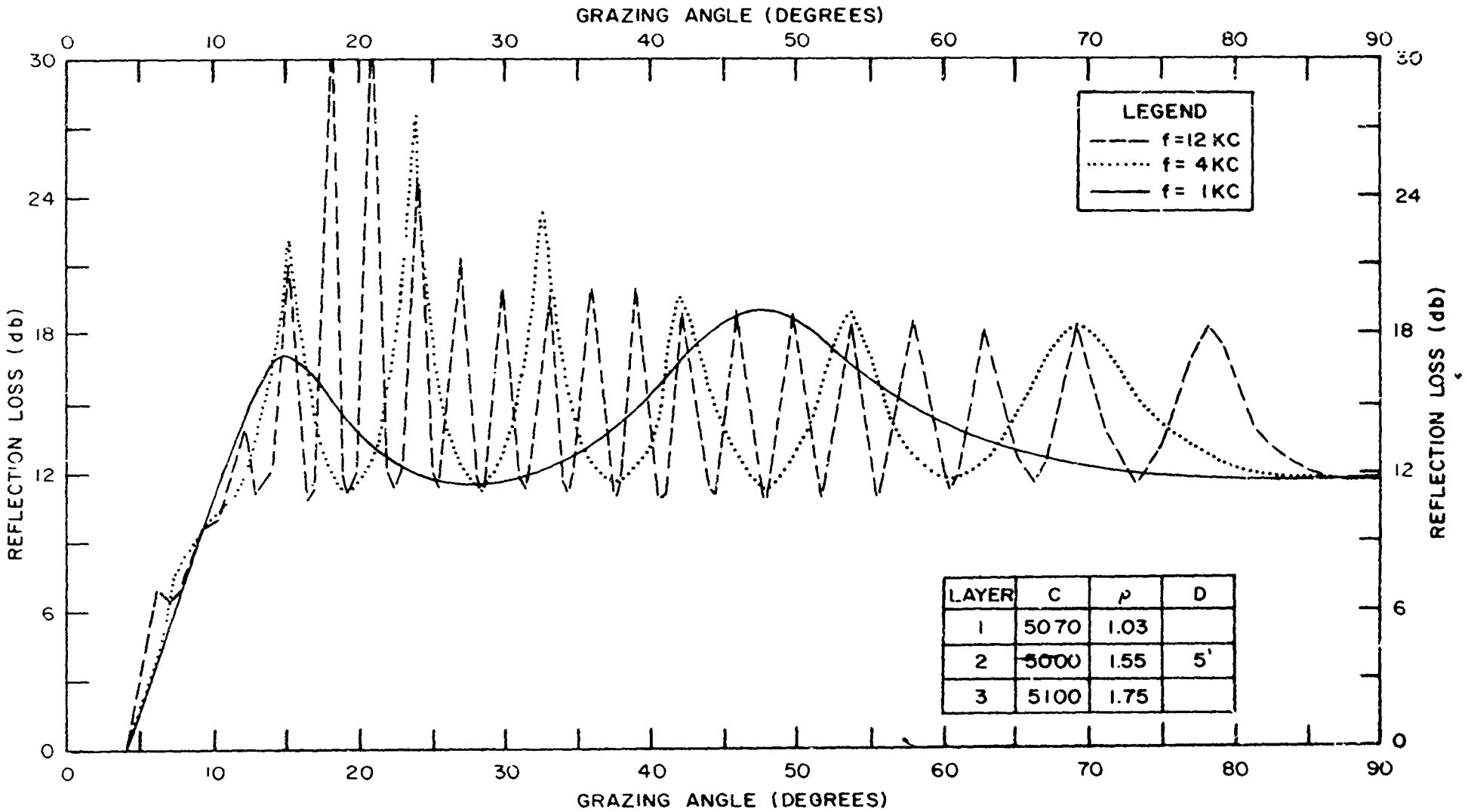

FIGURE 1. BOTTOM REFLECTION LOSS VERSUS GRAZING ANGLE AT 1, 4, AND 12 KC FOR $C_3 > C_1 > C_2$.

0-33-65

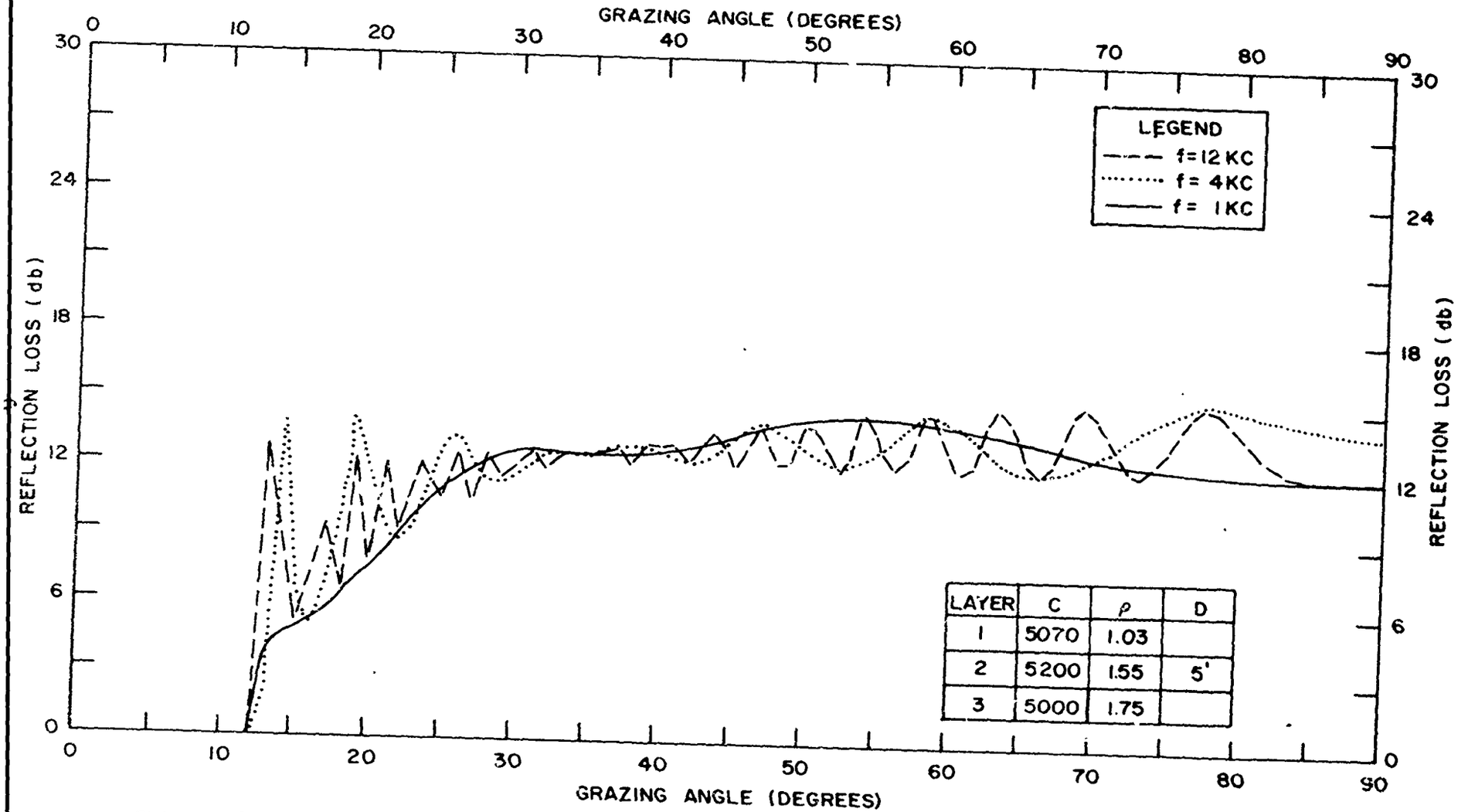

FIGURE 2. BOTTOM REFLECTION LOSS VERSUS GRAZING ANGLE AT 1, 4, AND 12 KC FOR $C_2 > C_1 > C_3$.

0-33-65

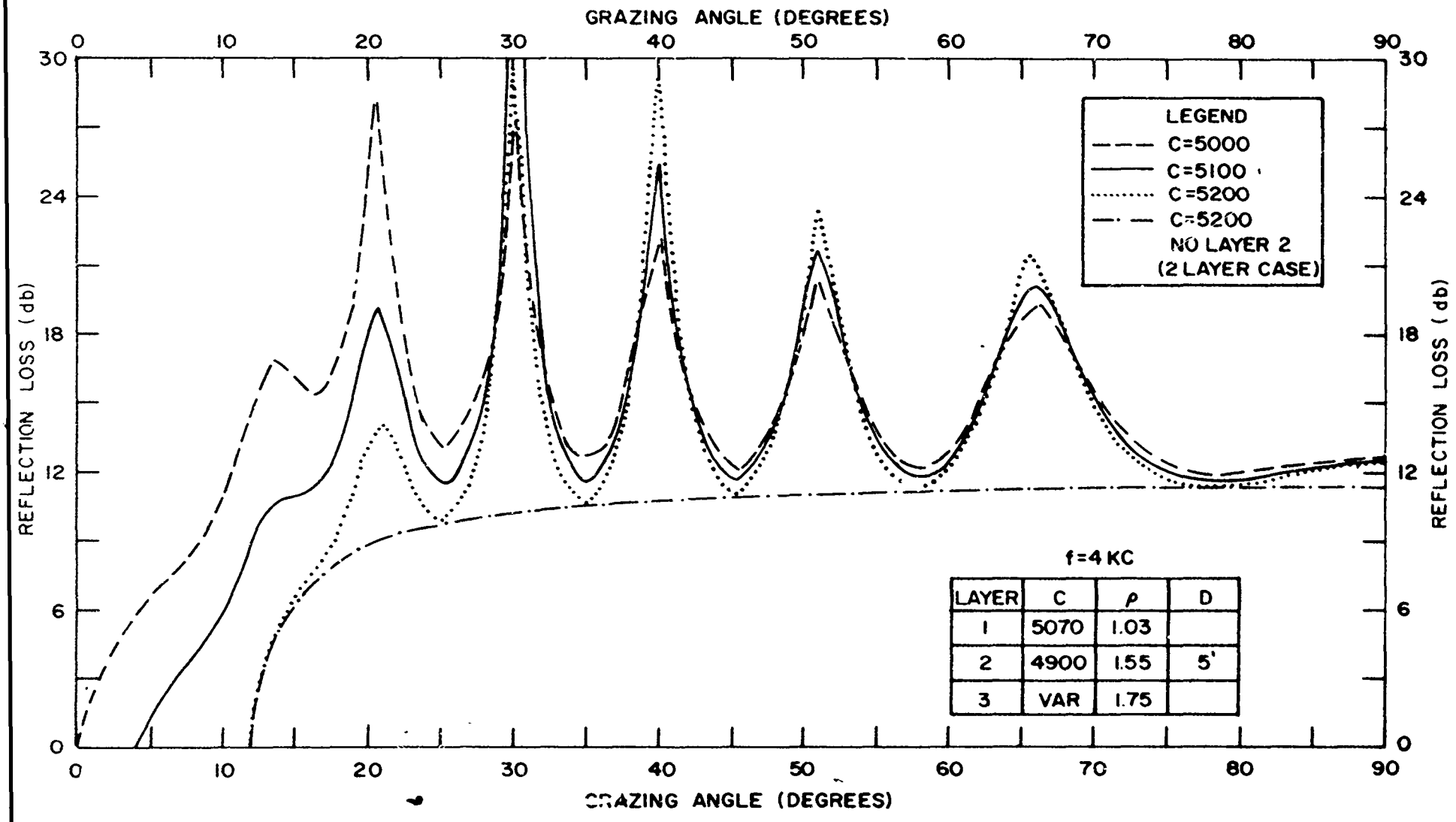

FIGURE 3. EFFECT OF C_3 ON BOTTOM LOSS FOR C_2 MINIMUM.

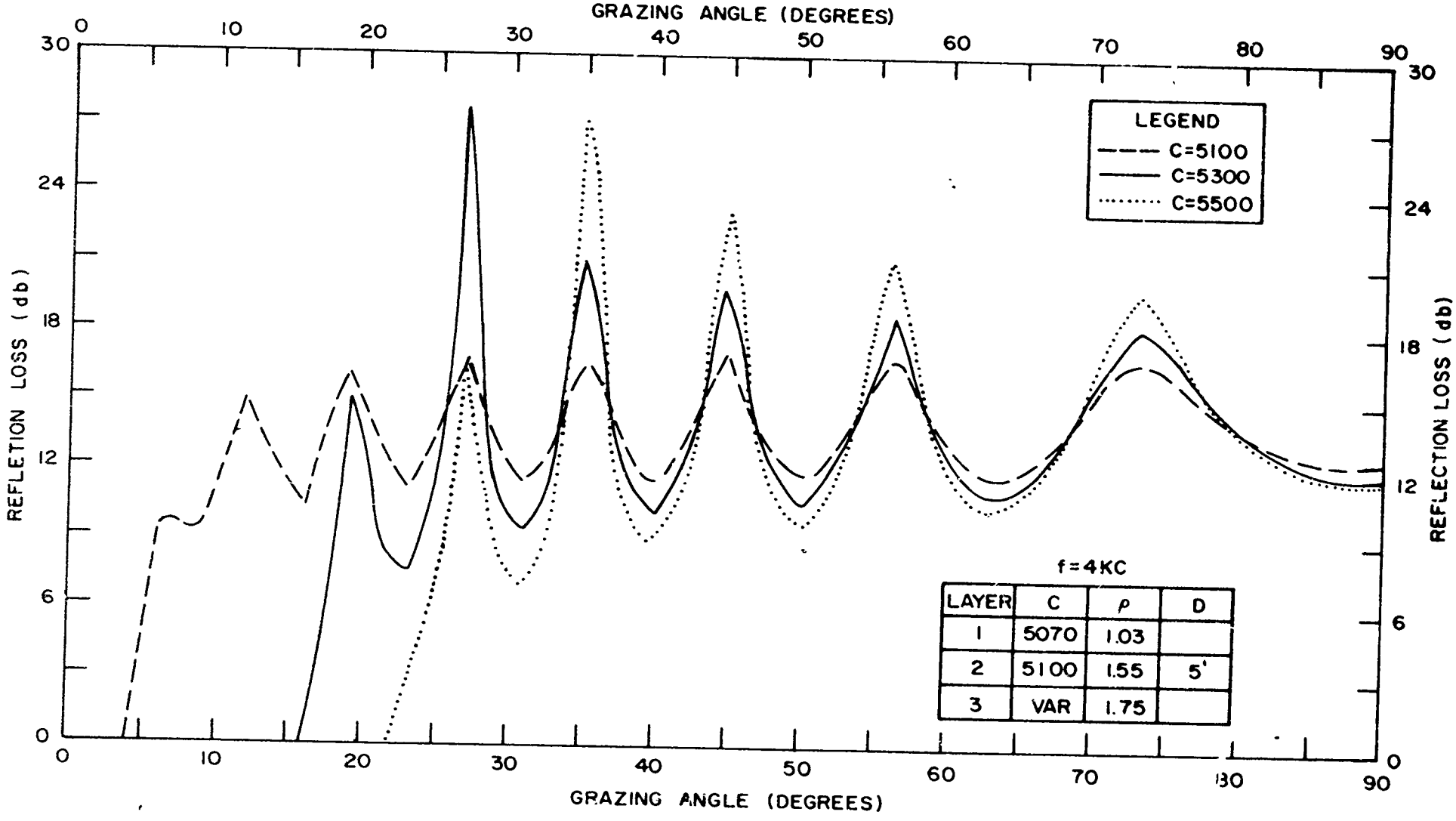

FIGURE 4. EFFECT OF C_3 ON BOTTOM LOSS FOR C_1 MINIMUM.

Figures 5 and 6 demonstrate the importance of layer 2 sound velocity (C_2) in computing reflection loss. In Figure 5 $C_2 \leq C_3$, but $\rho_2 C_2 < \rho_3 C_3$. As C_2 increases the number of oscillations increase, while the amplitude decreases. In the next illustration (Figure 6) the maximum velocity is determined by C_2 and the same dampening effect observed in Figure 2 can be seen again. This smoothing effect is seen to shift towards the higher grazing angles as C_2 increases. As in Figure 5 the amplitude of the fluctuations decreases as C_2 increases.

The influence of layer 2 thickness, in a three layer model, is shown in Figure 7. The layer thickness was varied with respect to wavelength. As the thickness increases from a quarter wavelength to 8 wavelengths the reflectivity curve changes from a smooth curve to one having 10 peaks. As expected, for normal incidence (90 degrees), a maximum loss value is obtained for the quarter wavelength and a minimum value for the half wavelength layer.

Figure 8 illustrates the result of increasing the number of reflecting layers to five. As was the case in Figures 1 and 2 the fluctuations increase as the frequency increases; however, in this case the reflectivity curves are not nearly as orderly. This results from the interference effects produced by four reflecting interfaces as the grazing angle varies.

To illustrate the effect of absorption in the sediments on the bottom reflection curves, Shumway's (4) 20 to 40 kc absorption data were extrapolated according to a square root, first power, and square dependence on frequency. The results of this test are illustrated in Figures 9, 10, and 11. For the case of reflection with absorption there is no critical angle and the reflection never becomes total. This is illustrated in Figure 9 for 1 kc. Absorption not only eliminates the critical angle and increases the loss values for angles less than 30 degrees, but also tends to dampen the fluctuations. This is most noticeable for the case of $a = 0.261$ decibel per foot, where the peak loss at 45 degrees of about 26 decibels for $a = 0$ decreases to about 19 decibels. As the absorption decreases this effect becomes less noticeable. Figure 10 depicts this same effect at 4 kc. Notice the extreme dampening for $a = 1.01$ decibels per foot. For $a = 0.108$ an additional peak has formed in the region less than the critical angle. Figure 11 represents a situation where D was increased to about 20 feet as compared to 5 feet in Figure 10. The number of oscillations has increased and the effect of absorption is noticeable by the dampened peaks. It appears that absorption tends to eliminate some of the effects of constructive and destructive interference, particularly for larger values of absorption.

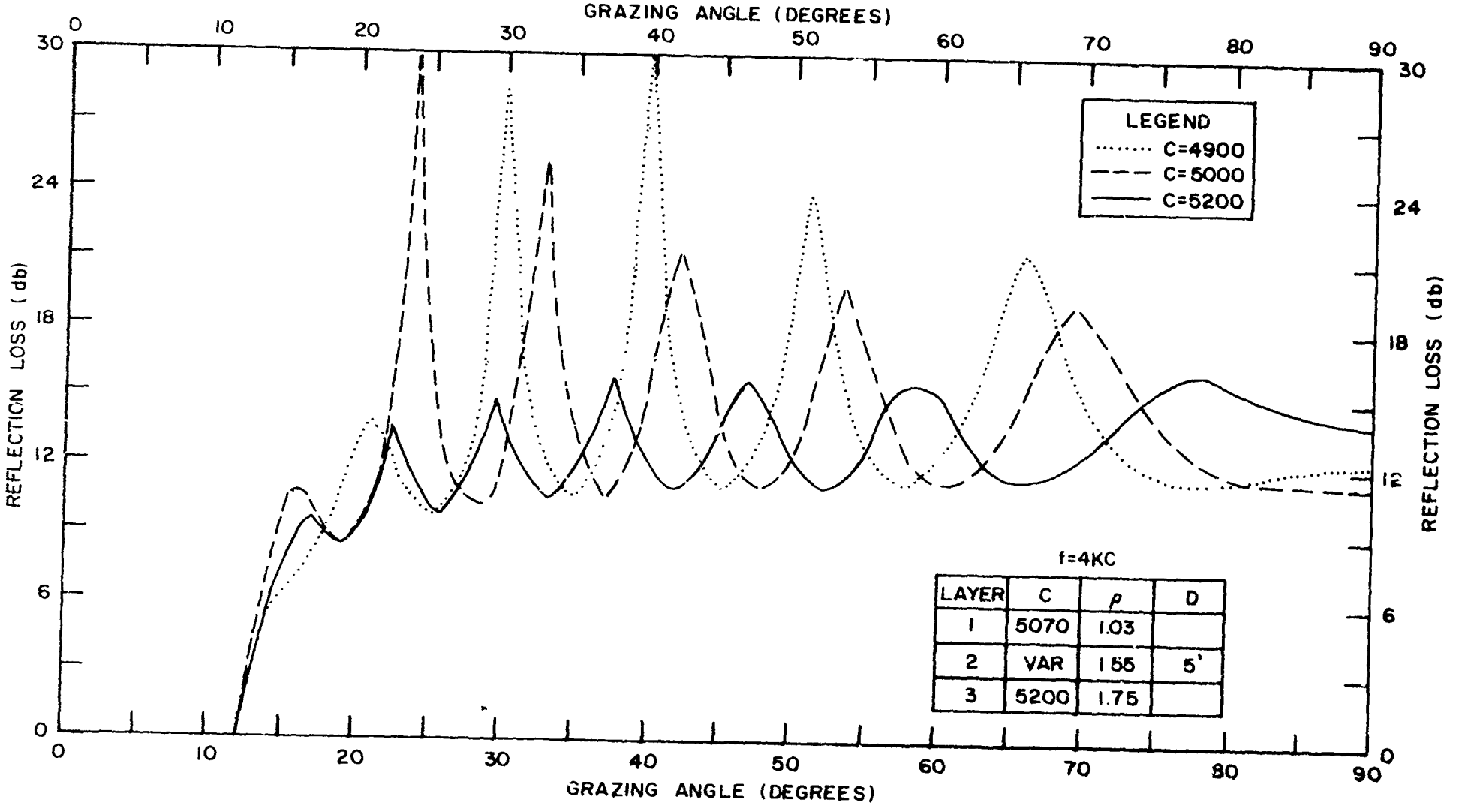

FIGURE 5. DEPENDENCE OF BOTTOM LOSS ON C_2.

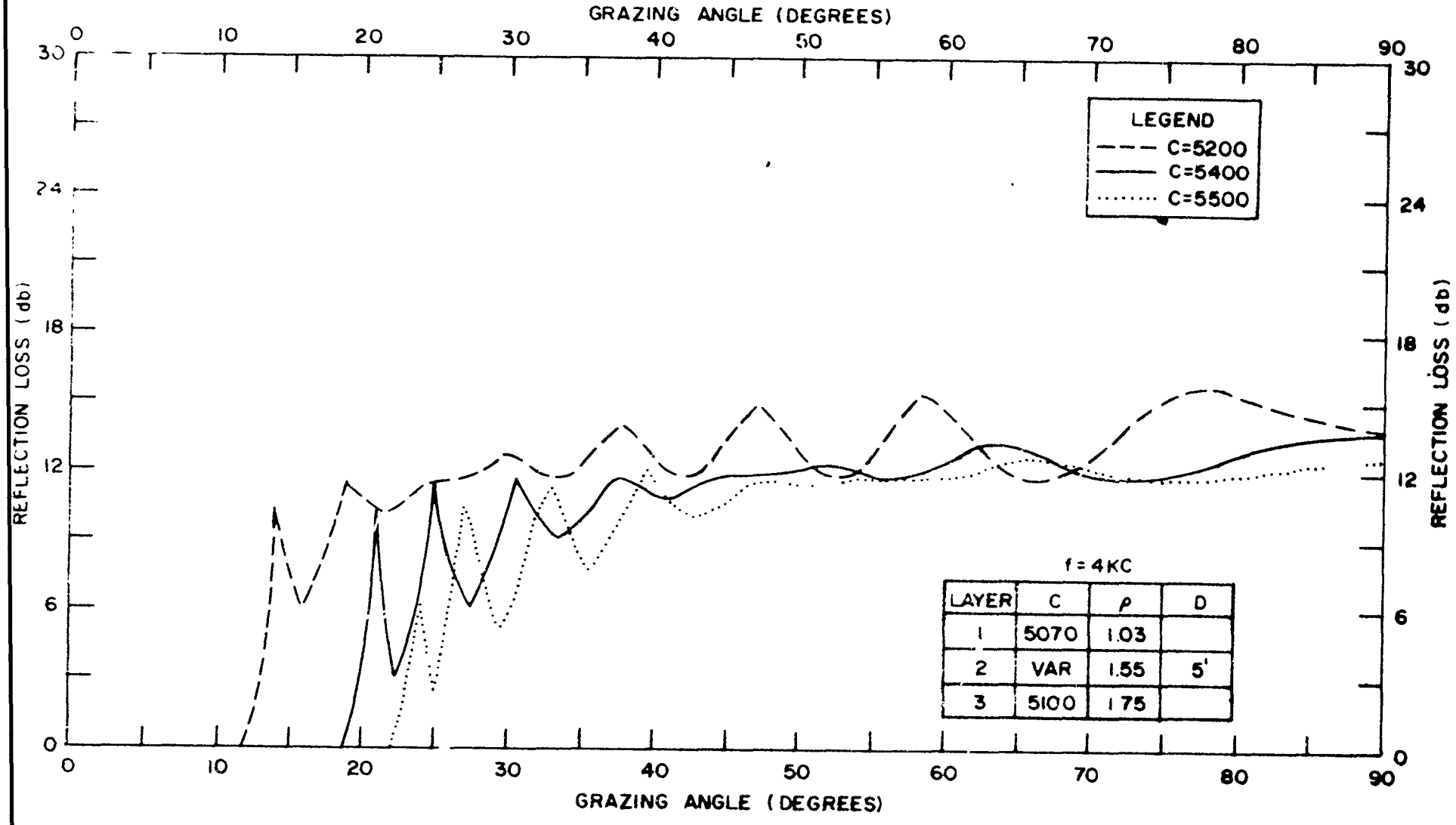

FIGURE 6. DEPENDENCE OF BOTTOM LOSS ON C_2.

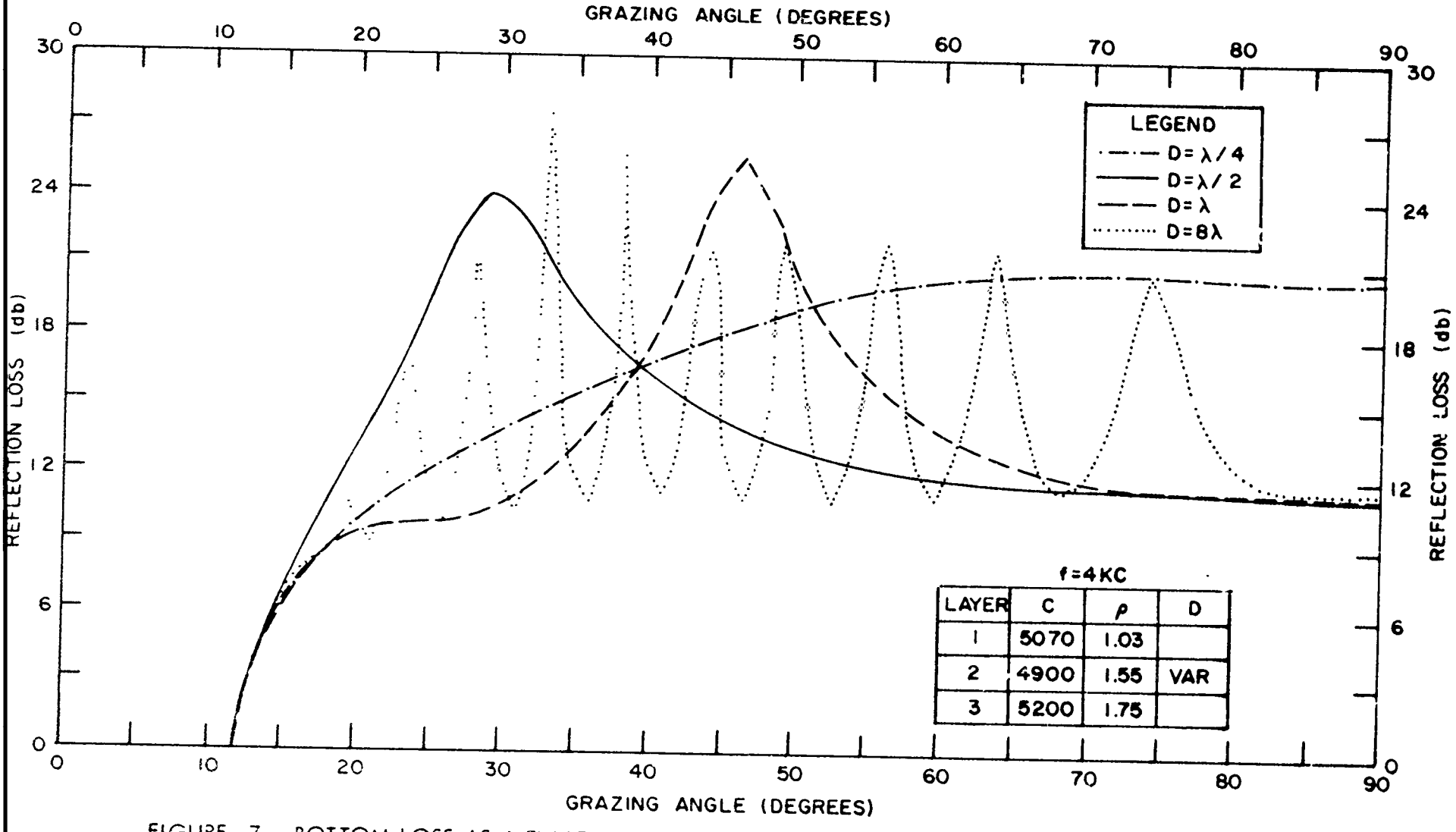

FIGURE 7. BOTTOM LOSS AS A FUNCTION OF GRAZING ANGLE FOR VARYING LAYER THICKNESS.

0-33-65

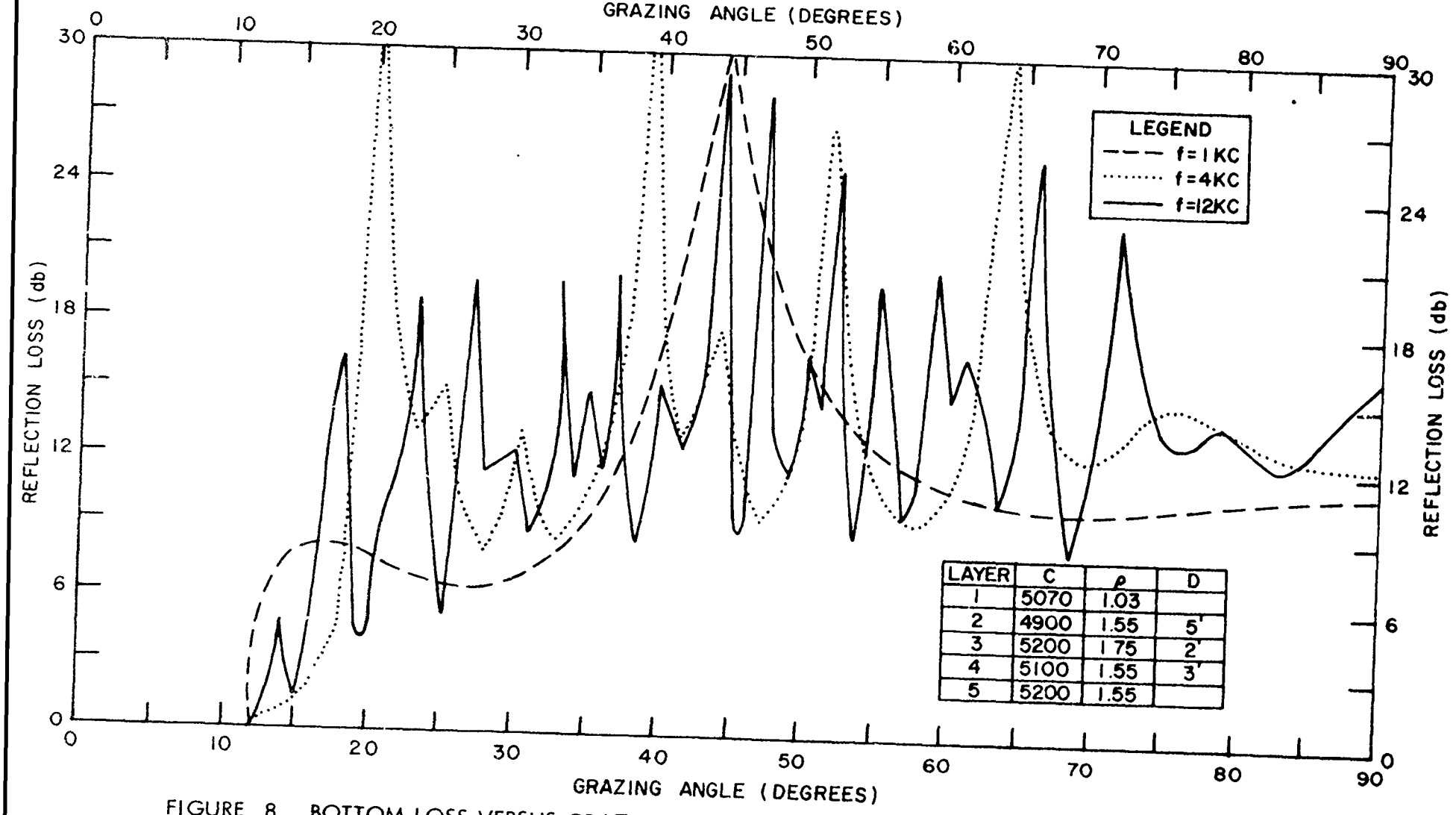

FIGURE 8. BOTTOM LOSS VERSUS GRAZING ANGLE AT 1, 4, AND 12 KC FOR A FIVE LAYER MODEL.

0-33-65

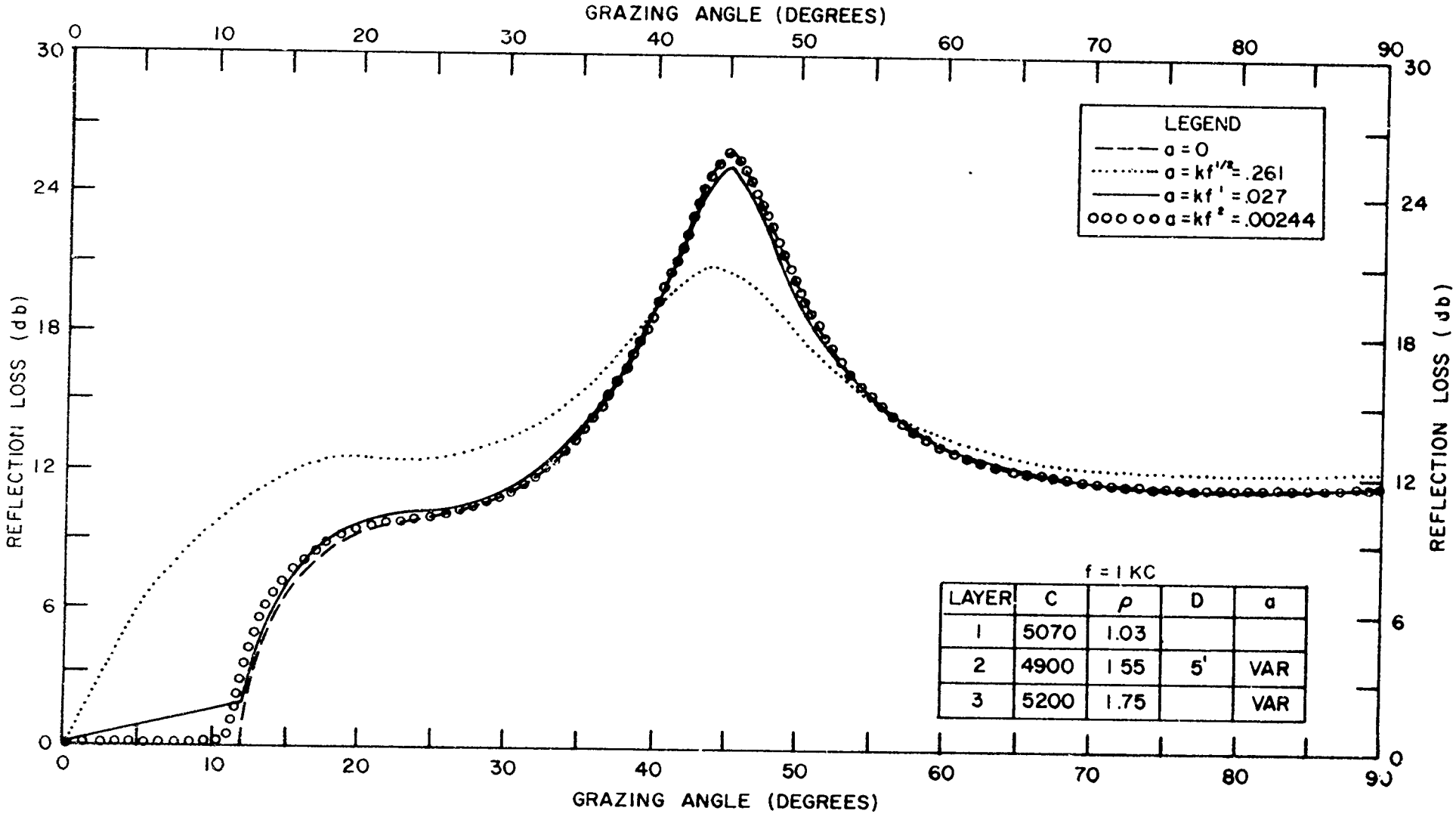

FIGURE 9. EFFECT OF ABSORPTION AT 1 KC ON BOTTOM LOSS.

0-53-65

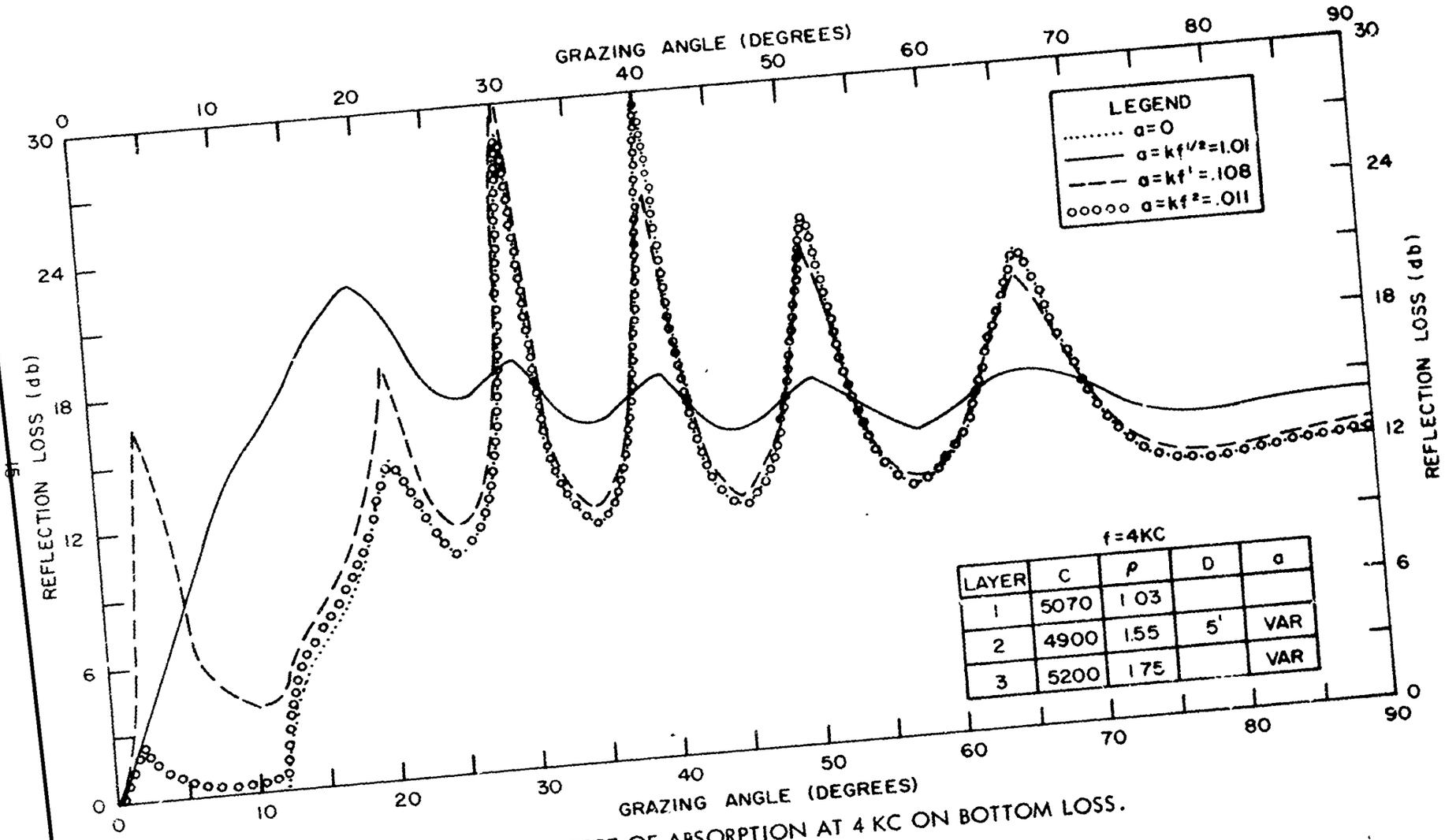

FIGURE 10. EFFECT OF ABSORPTION AT 4 KC ON BOTTOM LOSS.

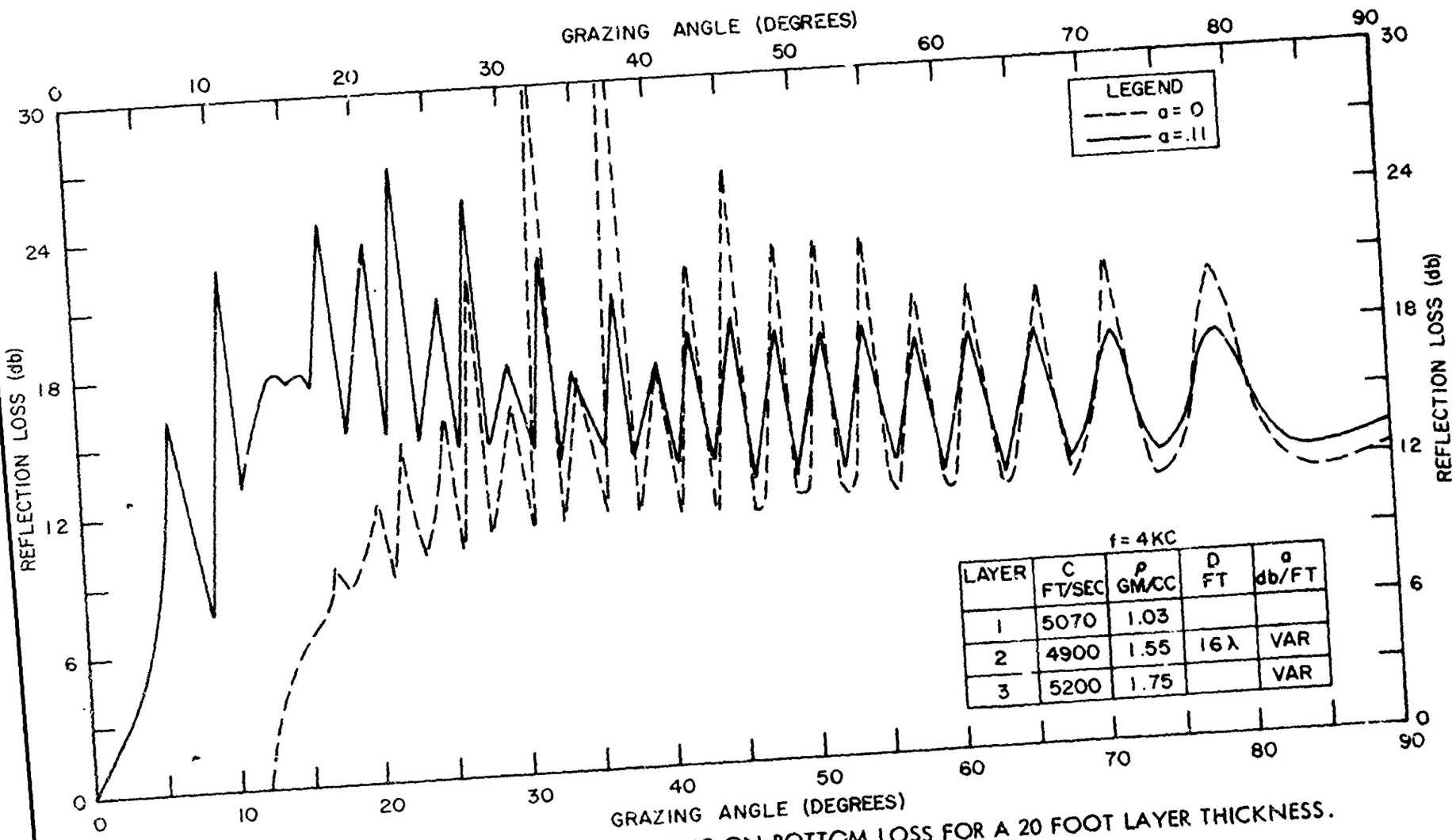

FIGURE 11. EFFECT OF ABSORPTION AT 4 KC ON BOTTOM LOSS FOR A 20 FOOT LAYER THICKNESS.

COMPARISON WITH EXPERIMENTAL DATA

In an attempt to establish the usefulness of the layered model for predicting reflection loss a comparison was made of measured loss values obtained in a water depth of about 2800 fathoms, in the Hatteras Abyssal Plain, with values computed from a short sediment core. A 2.5 foot core was taken at the location of a set of 6 kc bottom loss measurements made with explosive sound sources. The sediment grain size, porosity, density and various other physical properties were measured directly from the core. The Shumway semi-empirical relationship between porosity and velocity was used to compute sediment sound velocities. As indicated by Hamilton (6) these velocities were then corrected for the differences in temperature and pressure between Shumway's laboratory measurements and in situ conditions. Wilson's (7) tables for the speed of sound in sea water were used to make this correction. Absorption values were extrapolated from Shumway's high frequency data according to the first power frequency relation used by Mackenzie (8) and Cole (9). The measured density and estimated acoustic properties were then used to establish five thin layers for use in the model.

A comparison of the predicted and measured loss values at 6 kc is presented in Figure 12. Except at a grazing angle of 70 degrees the overall agreement appears to be good. The measured values represent the reflection loss at the water-sediment interface and the short core used for the computations should be adequate due to the extremely short pulse of the explosive sound source.

A similar comparison of computed and measured losses was made for a set of 3.5 kc measurements made in about 2800 fathoms of water in the Sohm Abyssal Plain. A short core was also used for the computations and the results are presented in Figure 13. The overall agreement between the computed and measured loss values appears to be quite good.

Other unpublished comparisons do not always exhibit such agreement; however, this does not necessarily suggest a deficiency in the theory or model, but may very well indicate that not enough is known about the exact relationships between the acoustic and physical properties of bottom sediments. While the studies presented in references 4, 5, and 6 are excellent studies one has only to compare the results of each to see that differences exist between the various environments sampled and that a universal relationship between the acoustic and physical properties of bottom sediments probably does not exist.

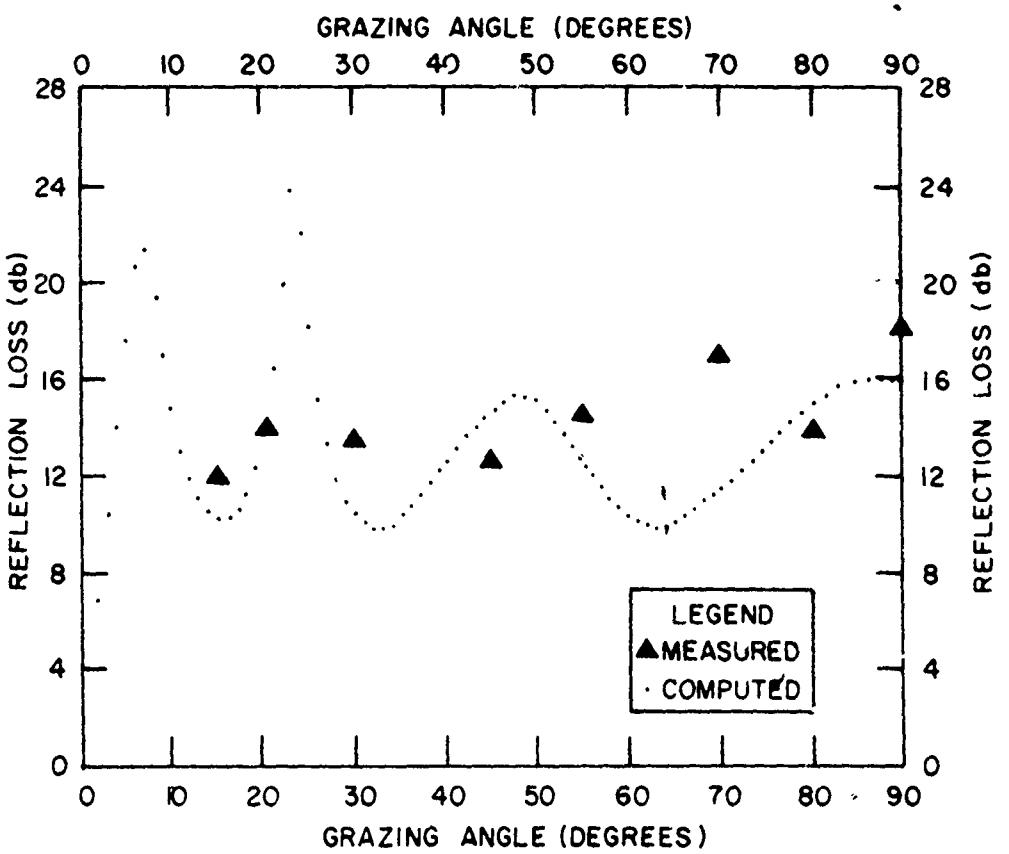

LAYER	C	ρ	D	α
1	5070	1 03		
2	5035	1.68	1.08'	.097
3	4979	1.60	.43	
4	5061	1.75	.16'	
5	5005	1.62	.36	
6	4946	1.50		

FIGURE 12. COMPARISON OF COMPUTED AND MEASURED REFLECTION LOSS AT 6 KC.

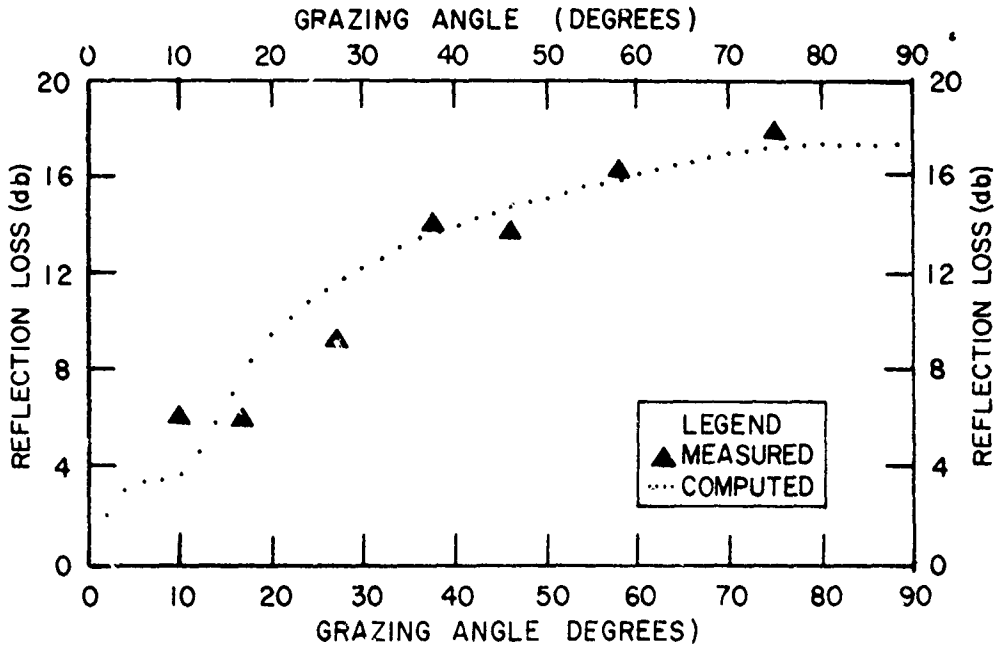

LAYER	C	ρ	D	α
1	5070	1.03		
2	4970	1.56	.3'	.17
3	5200	1.75		.39

FIGURE 13. COMPARISON OF COMPUTED AND MEASURED REFLECTION LOSS AT 3.5 KC.

SUMMARY

A computer model has been developed to permit systematic theoretical investigations to aid in the interpretation and prediction of ocean bottom reflectivity. In addition, such a model can be of value in planning acoustic measurement programs. The layered ocean bottom model can be used to explain the effect of frequency, layering, and sediment properties on bottom reflection loss as a function of grazing angle.

Theoretical computations can be used for interpreting acoustic data for the purpose of defining the acoustic properties of bottom sediments; however, extreme care must be exercised when so doing, as it is apparent that various combinations of sound velocity, density, absorption, and layer thickness can produce the same reflectivity curve.

Limited comparisons of computed and measured reflectivity in abyssal plain regions have shown that experimental data are consistent with a model that considers the ocean bottom to be flat, absorbing, layered, and fluid. The usefulness of the model for predicting bottom reflectivity is limited by our knowledge of the exact properties of the ocean bottom.

REFERENCES

1. Haskell, N. A., 1953, The dispersion of surface waves on multilayered media, Bulletin of the Seismological Society of America, v. 43, no. 12, pp. 17-34.

2. Alpine Geophysical Associates, Inc., 1964, Acoustic and geophysical survey of bottom and subbottom reflectivity, sponsored by U. S. Naval Oceanographic Office, H. O. 17416-1, Contract No. N62306-1442.

3. Hamilton, E. L., Shumway, G., Menard, H. W., and Shipek, C. J., 1956, Acoustic and other physical properties of shallow-water sediments off San Diego, Journal of the Acoustical Society of America, v. 28, no. 1, pp. 1-15.

4. Shumway, G., 1960, Sound speed and absorption studies of marine sediments by a resonance method, Parts I and II, Geophysics, v. 25, nos. 2 and 3, pp. 451-467 and 659-682.

5. Sutton, G. H., Berckheimer, H., and Nafe, J. E., 1957, Physical analysis of deep sea sediments, Geophysics, v. 22, no. 4, pp. 779-812.

6. Hamilton, E. L., 1963, Sediment sound velocity measurements made in situ from Bathyscaphe Trieste, Journal of Geophysical Research, v. 68, no. 21, pp. 5991-5998.

7. Wilson, W. D., 1959, Tables for the speed of sound in distilled water and in sea water, U. S. Naval Ordnance Report, No. 6747, 19 pp.

8. Mackenzie, K. V., 1960, Reflection of sound from coastal bottoms, Journal of the Acoustical Society of America, v. 32, no. 2, pp. 221-231.

9. Cole, B. F., 1964, Marine sediment attenuation and ocean-bottom reflected sound, paper E-1 presented at the 68th Meeting of the Acoustical Society of America.